Evaluation of anticancer activities varying ligand's substituents in Co(II/III)-picolyl phenolate derivatives: Synthesis, characterization, DFT, DNA cleavage and molecular docking studies

Abhimanyu Jana, Abhishek Aher, Paula Brandao,Pradip Bera, Saphy Sharda, Ujjwal Phadikar, Sunil Kumar Manna, Ajit Kumar Mahapatra and Pulakesh Bera*

Fig. S13. ^{1}H NMR of **C3.**

Fig. S14.^{1}H NMR of **L4.**

Fig. S15. ^{1}H NMR of **C4.**

Fig. S16. Mass spectrum of **L1** and **C1**

Fig. S17. Mass spectrum of **L2** and **C2**

Fig. S18. Mass spectrum of **L3** and **C3**

Fig. S19. Mass spectrum of **L4** and **C4**

Fig. S20. The hydrogen bonding and π-π interactions of **L1**.

Fig.S21. (a) Intermolecular hydrogen-bonding interactions of **1** (b) the supramolecular dimer formed by Type-A CH···π interaction of **1,** the supramolecular dimer formed by Type-B π···π interaction of **1** (c) the extended 2D supramolecular framework in crystallographic *ab* plane with polyhedron.

Fig. S22 The extended 1-D supramolecular sheet of complex **3**

Fig. S23. Frontier molecular energy diagram comparing the energy levels of **L1** and **1**.

Fig. S24. Frontier molecular energy diagram comparing the energy levels of **L2** and **2**.

Fig. S25. Frontier molecular energy diagram comparing the energy levels of **L3** and **3**.

Fig. S26. Frontier molecular energy diagram comparing the energy levels of **L4** and **4**.

Fig.S27. Cyclic voltammogram of **2**, **3** and **4**.

Fig. S28. A-C) Cytotoxicity effect of the compound with MTT assay: U-937, HEK 293T, and A549 cells were treated with different concentrations of L1−4, and its metal complexes 1, 2, 3, 4 for 72 hours to study the cytotoxic effect on cell lines from different cell origin. The mean cell death from three independent experiments was calculated and represented as % cell death compared to control (taken as zero) and doxorubicin (taken as positive control). D) The data obtained was transformed, normalized, and plotted as a non-linear regression curve to calculate IC_{50} values using Graphpad Prism 8. E) U-937, HEK 293T, and A549 cells were treated with different concentrations of doxorubicin for 72 h and MTT assay was carried out.

Fig. S29: The cell cycle profile studies of L1−4, and its metal complexes 1−4 with FACS.

Scheme

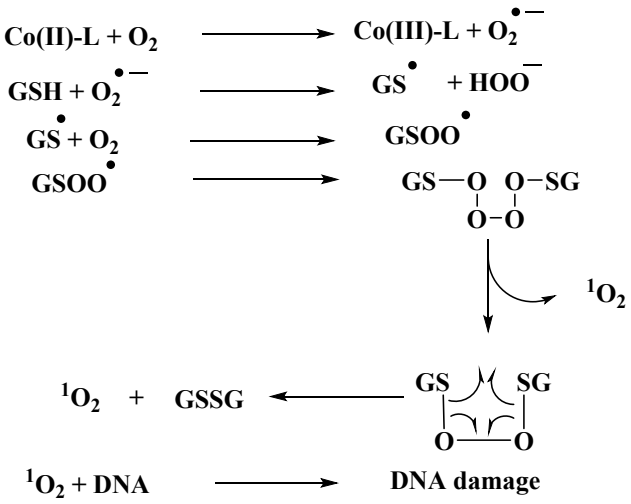

[Ref. H. Wefers and H. Sies, "Oxidation of glutathione by the superoxide radical to the disulfide and the sulfonate yielding singlet oxygen," ***European Journal of Biochemistry*, vol. 137, no. 1-2, pp. 29–36, 1983.]**

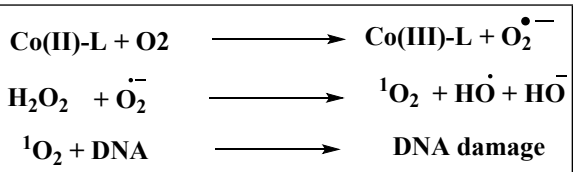

[Ref. Oxidative DNA damage of mixed copper(II) complexes with sulfonamides and 1,10-phenanthrolineCrystal structure of [Cu(*N*-quinolin-8-yl-*p*-toluenesulfona-midate) (1,10- 2phenanthroline). **Journal of Inorganic Biochemistry** 2003, **96,** 367–374]

Scheme S1: Mechanism of singlet oxygen generation by the complex in GSH and H_2O_2 medium.

Explanation: To determine the oxidative mechanism by which **1**–**3** induces DNA cleavage, nuclease activity was probed in the presence of reactive oxygen species (ROS) scavengers (NaN_3, glycerol, DMSO, and histidine) in GSH and H_2O_2 medium. NaN_3 displayed the greatest inhibitory effect, suggesting that singlet oxygen ($^1O_2$) is the major ROS intermediate formed during the DNA cleavage process. We propose that **1**–**3** reduces molecular oxygen (in solution) to superoxide, which generates singlet oxygen through Haber-Weiss reaction. The paramagnetic cobalt(II) ion in **1**–**3** could be responsible for singlet oxygen generation, via a photo-redox pathway in ambient light. (***Dalton Trans.***, 2018, **47**, 5755-5763)

TABLES

Table S1. FT-IR frequency (cm^{-1}) data of **L1-L4** and **1-4**.

Compound	ν_{O-H}	ν_{azide}	$\nu_{C=N}$ (azomethine)	ν_{C-N} (aromatic)	ν_{C-O} (phenolate)
L1	3180, 2931	-	1598	1482	1244
1	3217, 2994	-	1605	1489	1220
L2	-	-	1634	1485	1261
2	-		1630	1492	1250
L3	3442	-	1640	1482	1238
3	3442	-	1648	1490	1231
L4	3408	-	1633	1482	1238
4	-	2063	1654	1490	1224

Table S2. Crystal data and refinement parameters of the structure of **L1, L2**, **1**–**4.**

Crystal Data						
Compound	**L1**	**L2**	**1**	**2**	**3**	**4**
CCDC/CSD	2096735	2096736	2096741	2096740	2096738	2096739
Formula	$C_{13}H_{12}N_2O_2$	C24 H20 N2 O	$C_{13}H_{12}Cl_2CoN_2O_2$	$C_{26}H_{23}Cl_2CoN_3O$(1)	C_{16} H_{18} Cl_2 Co N_2 O_2	C_{21} H_{19} Co N_8 O_2
Formula Weight	228.25	352.42	358.08	523.30	400.15	474.37 g/mol
Crystal System	Monoclinic	Monoclinic	Monoclinic	Monoclinic	Monoclinic	orthorhombic
Space group	P 21/c	C 2/c	C 2/c	P 21/n	P 21/c	P 2_1 2_1 2_1
a, b, c [Å]	13.2747(8), 18.7979(11), 9.1742(5)	30.26(3), 4.659(5), 26.69(2)	20.068 (2), 11.4150 (11), 13.5735 (14)	11.3334 (6), 11.444 (6), 18.7309 (10)	13.3626(9), 8.7473(6), 14.7469(9)	9.9275(12) Å, 14.1515(16) Å ,14.8834(18) Å
α, β, γ [°]	90, 95.676(2), 90	90, 105.87(2), 90	90, 115.086(2), 90	90, 95.314(2), 90	90, 93.525(3), 90	90, 90, 90
V [Å^3]	2278.1(2)	3618(6)	2816.1(5)	2418.9(2)	1720.45(20)	2090.95(40)
Z	4	8	8	4	4	4
D(calc) [g/cm^3]	1.331	1.294	1.689	1.437	1.555 g/cm^3	1.507
μ(MoKα) [/mm]	0.092	0.080	1.599	0.954	1.317	0.858
F(000), F(000)′	960, 960.43	1488.0, 1488.56	1448.0, 1453.56	1076.0, 1078.86	820, 822.80	976, 977.67
h, k, lmax	16, 23,11	36,5,32	27, 15, 18	15, 15, 25	16, 10, 17	12, 17, 18
Crystal Size [mm]	0.24 x 0.12 x 0.04	0.28 x 0.08 x 0.02	0.22 x 0.18 x 0.04	0.22 x 0.12 x 0.03	0.32 x 0.2 x 0.06	0.28 x 0.12 x 0.04
Data Collection						

Temperature (K)	150	150	150	155	150	150
Radiation [Angstrom] MoKα	0.71073	0.71073	0.71073	0.71073	0.71073	0.71073
θ Max [Deg]	26.415	25.00	29.198	29.217	25.385	25.728
Data completeness	0.997	0.975	0.993	0.995	0.996	1.75
Tot., Uniq. Data, R(int)	28036, 4671, 0.058	15501, 3481, 0.075	41859, 3345, 0.038	31851, 5205, 0.033	24005, 3160, 0.043	19465, 3964, 0.094
Observed Data [I > 2.0 sigma(I)]	3750	2257	3345	5205	2764	3266
Refinements						
Nref, Npar	4683, 315	3571, 244	3833, 185	6571, 299	3172, 215	3979, 293
R, wR2, S	0.0413(3750), 0.1017(4671), 1.035	0.05(2257), 0.1578(3481), 1.038	0.0227(3345), 0.0593(3806), 1.059	0.0352(5205), 0.0776(6535), 1.077	0.0655(2764), 0.1771(3160), 1.191	0.0599(3266), 0.1693(3964), 1.095
Tmin, Tmax	0.987, 0.996	0.992, 0.998	0.715, 0.938	0.872, 0.972	0.691,0.924	0.884,0.966
	'w=1/[\s^2^(Fo^2^)+(0.0436P)^2^+0.6156P] where P=(Fo^2^+2Fc^2^)/3'	'w=1/[\s^2^(Fo^2^)+(0.0826P)^2^] where P=(Fo^2^+2Fc^2^)/3'	'w=1/[\s^2^(Fo^2^)+(0.0263P)^2^+2.7129P] where P=(Fo^2^+2Fc^2^)/3'	'w=1/[\s^2^(Fo^2^)+(0.0243P)^2^+1.5509P] where P=(Fo^2^+2Fc^2^)/3'	'w=1/[\s^2^(Fo^2^)+(0.0575P)^2^+12.8407P] where P=(Fo^2^+2Fc^2^)/3'	'w=1/[\s^2^(Fo^2^)+(0.0866P)^2^+1.9648P] where P=(Fo^2^+2Fc^2^)/3'

Table S3. Bond distances of **L1**, **L2**, and **1**−**4**.

L1					
Atoms	Length (Å)	Atoms	Length (Å)	Atoms	Length (Å)
O1A−C7A	1.3696(17)	O1B−C7B	1.3729(16)	N1A−C1A	1.335(2)
O1A−C6A	1.4216(16)	O1B−C6B	1.4174(15)	N1A−C5A	1.3357(17)
O2A−N2A	1.4064(16)	O2B−N2B	1.3999(15)	N2A−C13A	1.2705(18)
O2A−H2AA	0.93(2)	O2B−H2BB	0.94(2)	N1B−C1B	1.3374(19)
N1B−C5B	1.3405(17)	N2B−C13B	1.2674(18)		
L2					
Atoms	Length (Å)	Atoms	Length (Å)	Atoms	Length (Å)
O1—C7	1.368(3)	C3—C4	1.380(4)	C11—C12	1.387(3)
O1—C6	1.423(3)	C4—C5	1.384(3)	C14—C15	1.518(3)
N2—C13	1.276(3)	C5—C6	1.494(3)	C15—C16	1.370(3)
N2—C14	1.461(3)	C7—C12	1.387(3)	C15—C24	1.429(3)
N1—C1	1.335(3)	C7—C8	1.413(3)	C16—C17	1.411(3)
N1—C5	1.341(3)	C8—C9	1.392(3)	C17—C18	1.357(3)
C1—C2	1.374(4)	C8—C13	1.473(3)	C18—C19	1.419(3)
C2—C3	1.379(3)	C9—C10	1.381(3)	C19—C20	1.413(3)
1					
Atoms	Length (Å)	Atoms	Length (Å)	Atoms	Length (Å)
Co−N1	2.0449(12)	O1−C6	1.4356(16)	Co−Cl2	2.3334(4)
Co−N2	2.0582(12)	O2−N2	1.4007(15)	O1−C7	1.3838(16)
Co−Cl1	2.2639(4)	O2−H2A	0.876(9)	N1−C1	1.3549(17)
Co−O1	2.3039(10)	N1−C5	1.3443(18)	N2−C13	1.2817(19)
2					
Atoms	Length (Å)	Atoms	Length (Å)	Atoms	Length (Å)
Co−N1	2.0549(14)	N1−C5	1.345(2)	Co−O1	2.3220(12)
Co−N2	2.0657(14)	N1−C1	1.346(2)	O1−C7	1.373(2)
Co−Cl1	2.2851(5)	N2−C13	1.284(2)	O1−C6	1.433(2)

Co–Cl2	2.2862(5)	N2–C14	1.472(2)	N100–C101	1.143(4)
3					
Atoms	Length (Å)	Atoms	Length (Å)	Atoms	Length (Å)
Co1—N2	2.059(5)	Co1—Cl1	2.2883(17)	Co1—O1	2.299(4)
Co1—N1	2.064(5)	Co1—Cl2	2.2918(16)	O1—C7	1.370(7)
O2—H2A	0.904(10)	O2—C15	1.452(9)	N1—C5	1.349(7)
N1—C1	1.352(8)	N2—C13	1.284(8)	N2—C14	1.472(8)
4					
Atoms	Length (Å)	Atoms	Length (Å)	Atoms	Length (Å)
Co–O1	1.849(5)	O2–C15	1.386(9)	N3–N4	1.190(9)
Co–N1	1.868(6)	O2–C16	1.420(10)	N4–N5	1.145(10)
Co–N2	1.908(7)	N1–C9	1.276(9)	N6–N7	1.173(12)
Co–N6	1.954(7)	N1–C2	1.491(9)	N7–N8	1.190(14)
Co–N3	1.971(6)	N2–C21	1.349(10)	O1–C1	1.397(10)
Co–O2	1.989(5)	N2–C17	1.359(10)		

Table S4. Bond angles of **L1**, **L2**, and **1**–**4**.

L1					
Atoms	Angle (°)	Atoms	Angle (°)	Atoms	Angle (°)
C7A–O1A–C6A	118.85(11)	O1A–C6A–C5A	108.13(11)	C1B–N1B–C5B	117.86(13)
N2A–O2A–H2AA	101.6(13)	O1A–C6A–H6A1	110.1	C13B–N2B–O2B	111.23(12)
C1A–N1A–C5A	117.91(13)	O1A–C6A–H6A2	110.1	N1B–C1B–C2B	123.34(14)
C13A–N2A–O2A	110.65(12)	O1A–C7A–C8A	124.67(13)	O1B–C6B–H6B1	110.1
N1A–C1A–C2A	123.48(14)	O1A–C7A–C12A	114.60(12)	N1B–C5B–C4B	122.49(13)
N1A–C1A–H1A	118.3	N2A–C13A–C12A	120.82(13)	N1B–C5B–C6B	114.30(12)
N1A–C5A–C4A	122.18(13)	N2A–C13A–H13A	119.6	O1B–C6B–H6B2	110.1
N1A–C5A–C6A	114.39(12)	N2B–O2B–H2BB	101.8(13)	O1B–C6B–C5B	108.15(11)
C7B–O1B–C6B	118.03(10)	N1B–C1B–H1B	118.3	N2B–C13B–C12B	120.96(13)
N2B–C13B–H13B	119.5	O1B–C7B–C12B	115.65(12)		
L2					
Atoms	Angle(°)	Atoms	Angle(°)	Atoms	Angle(°)
C7—O1—C6	118.55(18)	N2—C13—C8	120.9(2)	O1—C6—H6B	110.000
C13—N2—C14	115.7(2)	N2—C13—H13	119.600	C5—C6—H6B	110.000
C1—N1—C5	117.1(2)	C8—C13—H13	119.600	H6A—C6—H6B	108.400
N1—C1—C2	124.7(2)	N2—C14—C15	112.18(19)	O1—C7—C12	125.27(19)
N1—C1—H1	117.600	N2—C14—H14A	109.200	O1—C7—C8	114.9(2)
N1—C5—C4	122.0(2)	N2—C14—H14B	109.200	O1—C6—C5	108.27(19)
N1—C5—C6	114.6(2)	C4—C5—C6	123.3(2)	O1—C6—H6A	110.000
1					

Atoms	Angle(°)	Atoms	Angle(°)	Atoms	Angle(°)
N1−Co−N2	136.99(5)	C7−O1−C6	115.86(10)	N1−C1−C2	122.74(14)
N1−Co−Cl1	106.63(4)	C7−O1−Co	126.33(8)	N1−C1−H1	118.6
N2−Co−Cl1	107.30(4)	C6−O1−Co	111.20(8)	N2−C13−C12	125.63(13)
N1−Co−O1	74.74(4)	N2−O2−H2A	103.0(14)	O1−C7−C12	116.97(12)
N2−Co−O1	77.96(4)	C5−N1−C1	118.18(12)	N1−C5−C4	122.23(13)
Cl1−Co−O1	92.80(3)	C5−N1−Co	119.86(9)	N1−C5−C6	118.88(12)
N1−Co−Cl2	100.46(3)	C1−N1−Co	121.40(10)	O1−C6−C5	109.29(11)
N2−Co−Cl2	92.85(4)	C13−N2−O2	110.76(12)	O1−C6−H6A	109.8
Cl1−Co−Cl2	108.794(16)	C13−N2−Co	131.88(10)	O1−C6−H6B	109.8
O1−Co−Cl2	158.27(3)	O2−N2−Co	116.10(9)	O1−C7−C8	122.66(12)
2					
Atoms	Angle(°)	Atoms	Angle(°)	Atoms	Angle(°)
N1−Co−N2	119.82(6)	C7−O1−C6	118.43(13)	N1−C5−C4	121.98(17)
N1−Co−Cl1	109.87(4)	C7−O1−Co	117.63(10)	N1−C5−C6	116.79(15)
N2−Co−Cl1	117.13(4)	C6−O1−Co	108.71(10)	N2−C13−C12	125.75(16)
N1−Co−Cl2	102.65(4)	C5−N1−C1	118.44(15)	N2−C13−H13	117.1
N2−Co−Cl2	100.53(4)	C5−N1−Co	120.57(12)	O1−C6−H6A	110.5
Cl1−Co−Cl2	103.71(2)	C1−N1−Co	120.99(12)	N100−C101−C102	179.3(3)
N1−Co−O1	72.28(5)	C13−N2−C14	116.62(15)	O1−C6−H6B	110.5
N2−Co−O1	76.10(5)	C13−N2−Co	126.86(12)	O1−C7−C12	115.35(15)
Cl1−Co−O1	85.50(3)	C14−N2−Co	116.30(11)	O1−C6−C5	106.11(13)
Cl2−Co−O1	170.66(3)	N1−C1−C2	122.18(19)	N1−C1−H1	118.9
3					
Atoms	Angle(°)	Atoms	Angle(°)	Atoms	Angle(°)
N2—Co1—N1	121.25(18)	N1—Co1—Cl1	103.05(14)	N1—Co1—Cl2	107.46(14)
N2—Co1—Cl1	102.03(15)	N2—Co1—Cl2	118.69(15)	Cl1—Co1—Cl2	100.64(6)
N2—Co1—O1	77.49(17)	Cl1—Co1—O1	174.36(11)	C1—N1—Co1	124.5(4)
N1—Co1—O1	72.79(17)	Cl2—Co1—O1	84.39(11)	C5—N1—Co1	117.8(4)
C7—O1—Co1	119.1(3)	C6—O1—Co1	106.5(3)	C14—N2—Co1	116.6(4)
C13—N2—Co1	126.7(4)	O1—C7—C12	115.2(5)	O1—C7—C8	123.9(5)
4					
Atoms	Angle (°)	Atoms	Angle(°)	Atoms	Angle(°)
O1−Co−N1	87.6(3)	N2−Co−N3	92.0(3)	C2−N1−Co	112.2(5)
O1−Co−N2	92.9(3)	N6−Co−N3	172.6(3)	C9 −N1−Co	125.6(5)
N1−Co−N2	178.5(2)	O1−Co−O2	176.9(3)	C21−N2−Co	125.9(6)
O1−Co−N6	93.3(3)	N1−Co−O2	95.4(2)	C17−N2−Co	115.3(5)
N1−Co−N6	89.7(3)	N2−Co−O2	84.0(3)	N4−N3−Co	120.5(5)
N2−Co−N6	88.9(3)	N6−Co−O2	86.9(3)	N7−N6−Co	118.2(7)
O1−Co−N3	94.0(2)	N3−Co−O2	85.9(3)	C15−O2−Co	126.2(5)
N1−Co−N3	89.4(3)	C1−O1−Co	109.0(4)	C16−O2−Co	114.2(4)

Table S5. BVS calculation.BVS calculation for **4:**

r_o	Bond type	Distance(r_{ij})	S_{ij}
1.68	Co1—N1	1.868(6)	0.6015
1.68	Co1—N2	1.908(7)	0.5399
1.68	Co1—N3	1.971(6)	0.4551
1.68	Co1—N6	1.954(6)	0.4768
1.68	Co1—O1	1.849(5)	0.852
1.68	Co1—O2	1.989(5)	0.584

Note: The bond valence sum (BVS) method is an empirical means of estimating the oxidation state of a metal ion from metal-ligand distances. The method is predicated on the assumption that the length of any given metal-ligand bond is related via a simple expression to the oxidation state of the metal ion.The expression is: $\mathbf{BVS=\sum S_{ij}=\sum e^{(r_o-r_{ij})/0.37}}$

Where, r_{ij} is the experimental bond length, r_0 is an empirical parameter associated with the metal in a given oxidation state and the type of coordinating atom, and $\mathbf{S_{ij}}$ is the bond valence value for the j^{th} bonded atom to the i^{th} metal.

Thus $\sum S_{ij}$ value=3.507 indicates cobalt atom in complex **4** has +3 oxidation state.

Table S6. Calculated Frontier Molecular Orbital energies (eV) for **L1-L4** and **1-4**.

Basis set	**L1**	**L2**	**L3**	**L4**	**1**	**2**	**3**	**4**
$\mathbf{E_{HOMO}}$**, eV**	–5.9780	–5.4486	–5.38	–5.23	–14.3530	–12.7167	–14.05	–15.82
$\mathbf{E_{LUMO}}$**, eV**	–1.1472	–1.2540	–1.15	–0.81	–13.4714	–8.7216	–12.52	–15.17
$\mathbf{\Delta E_{Gap}}$**, eV**	4.8308	4.1946	4.23	4.42	0.8816	3.9944	1.53	0.65
$\mathbf{E_{HOMO-1}}$**, eV**	–6.6052	–6.1149	–6.03	–5.75	–14.6850	–13.0027	–14.32	–16.44

E_{LUMO+1}, eV	–0.8144	–1.0095	–0.65	–0.50	–13.0468	–8.5640	–9.61	–13.21
IP, eV	5.9780	5.4486	5.38	5.23	14.3530	12.7167	14.05	15.82
EA, eV	1.1472	1.2540	1.15	0.81	13.4714	8.7216	12.52	15.17
η, eV	2.4154	2.0973	2.115	2.21	0.4408	1.9972	0.76	0.325
χ, eV	3.35626	3.3513	3.265	3.02	13.9122	10.7196	13.285	15.495
σ, eV	0.414	0.476	0.472	0.452	2.268	0.5		3.076
μ_p, eV	−3.35626	−3.3513	-3.265	-3.02	−13.9122	−10.7196		–15.495

[E_{TOTAL}: Total energy; E_{HOMO}: HOMO energy; E_{LUMO}: LUMO energy values. $\Delta E_{Gap} = (E_{LUMO} – E_{HOMO})$; IP: Ionization potential; EA: Electron affinity; η: Absolute hardness, (I – A)/2. χ: Electronegativity, (I + A)/2. σ: Softness, 1/η. μ_p: Chemical potential, – (I + A)/2].

A. Spectroscopy (UV-Visible, FTIR and ^{1}H-NMR)

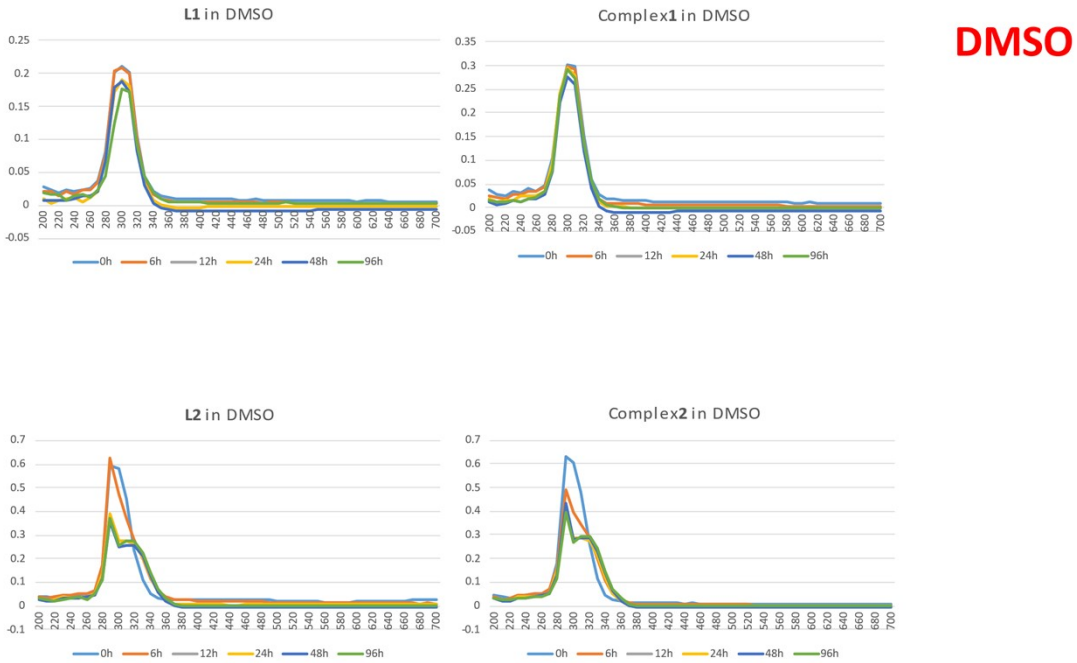

DMSO

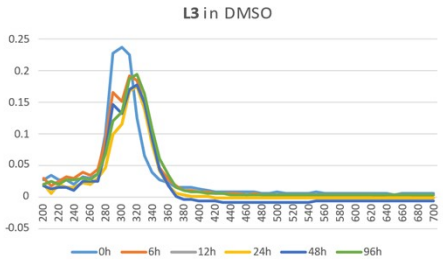
L3 in DMSO
0h 6h 12h 24h 48h 96h

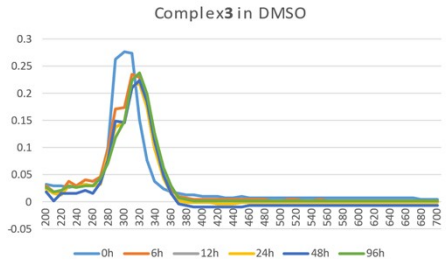
Complex3 in DMSO
0h 6h 12h 24h 48h 96h

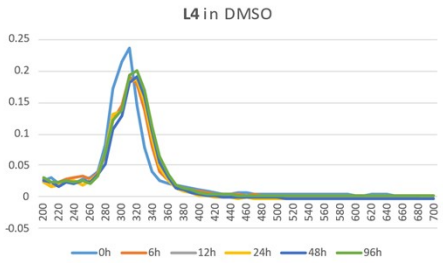
L4 in DMSO
0h 6h 12h 24h 48h 96h

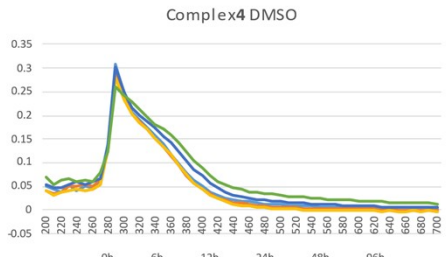
Complex4 DMSO

RPMI

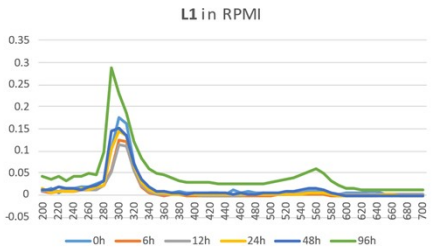
L1 in RPMI
0h 6h 12h 24h 48h 96h

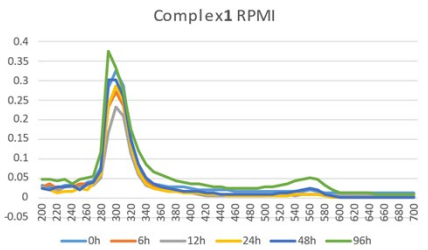
Complex1 RPMI
0h 6h 12h 24h 48h 96h

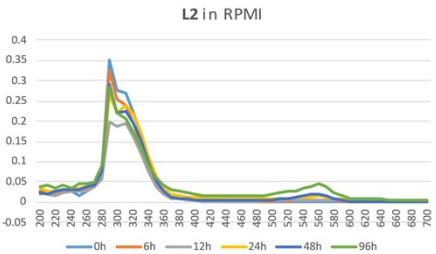
L2 in RPMI
0h 6h 12h 24h 48h 96h

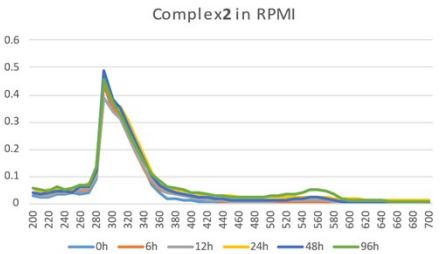
Complex2 in RPMI
0h 6h 12h 24h 48h 96h

RPMI

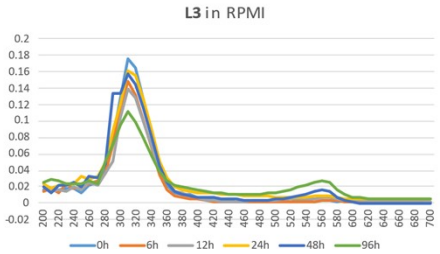
L3 in RPMI
0h 6h 12h 24h 48h 96h

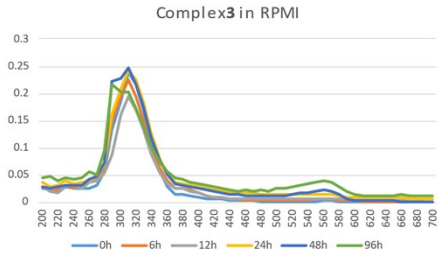
Complex3 in RPMI
0h 6h 12h 24h 48h 96h

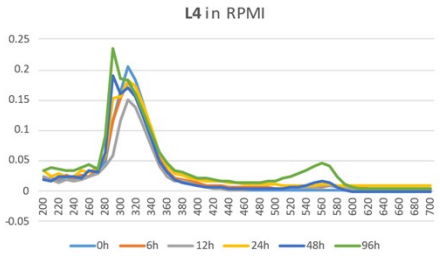
L4 in RPMI
0h 6h 12h 24h 48h 96h

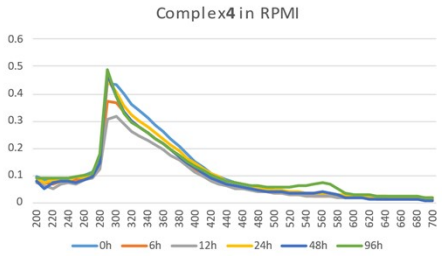
Complex4 in RPMI
0h 6h 12h 24h 48h 96h

PBS

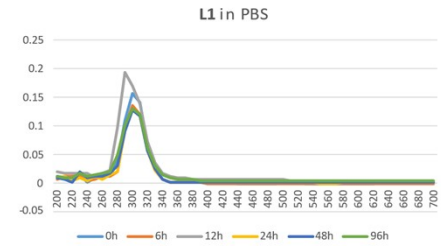
L1 in PBS
0h 6h 12h 24h 48h 96h

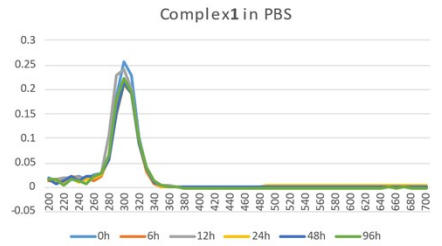
Complex1 in PBS
0h 6h 12h 24h 48h 96h

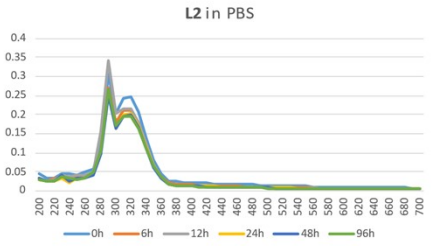
L2 in PBS
0h 6h 12h 24h 48h 96h

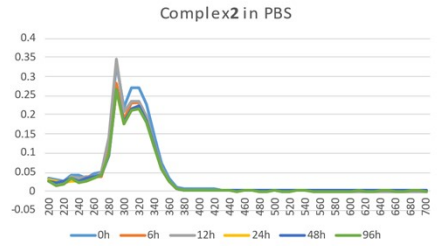
Complex2 in PBS
0h 6h 12h 24h 48h 96h

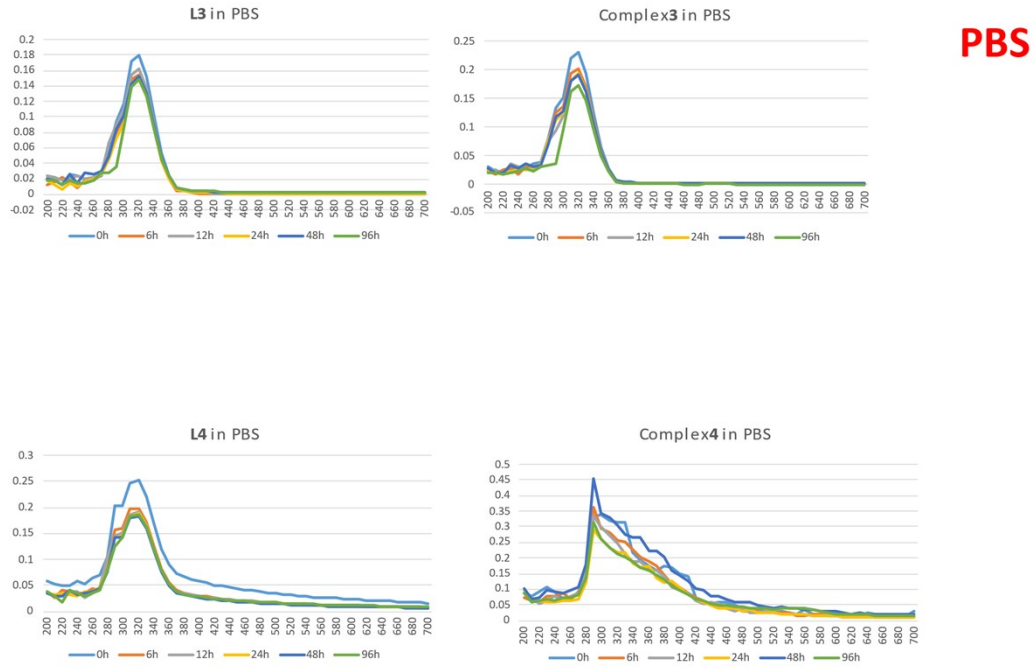

Fig. S1: UV-Vis spectra (0-96 hours) of **L1-L4** and **1-4** in DMSO, RPMI and PBS.

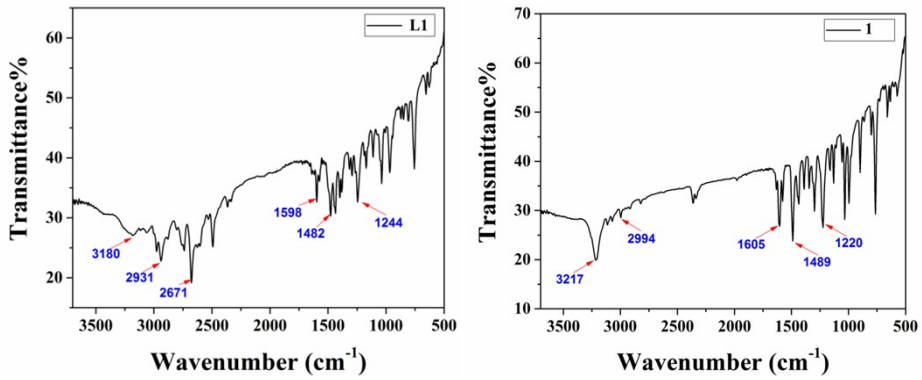

Fig. S2. IR spectrum of **L1** and **1.**

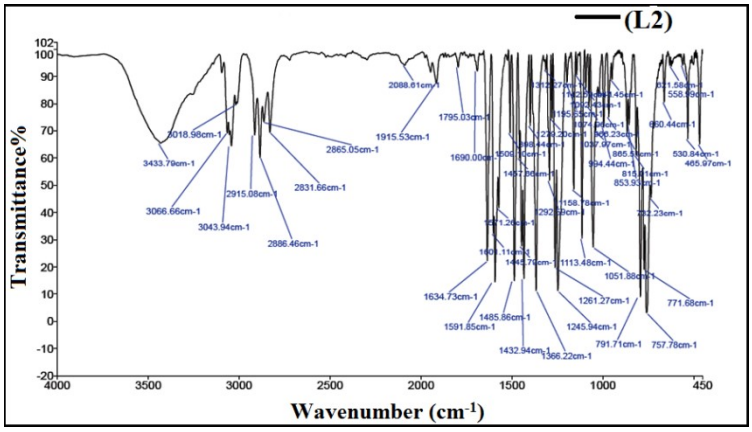

Fig. S3. IR spectrum of **L2.**

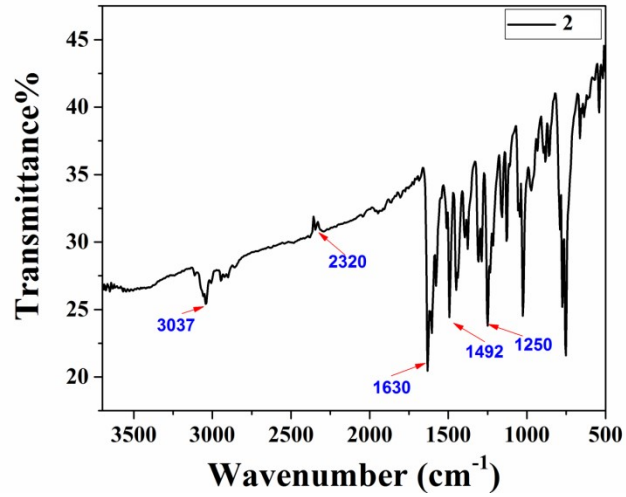

Fig. S4. IR spectrum of **2.**

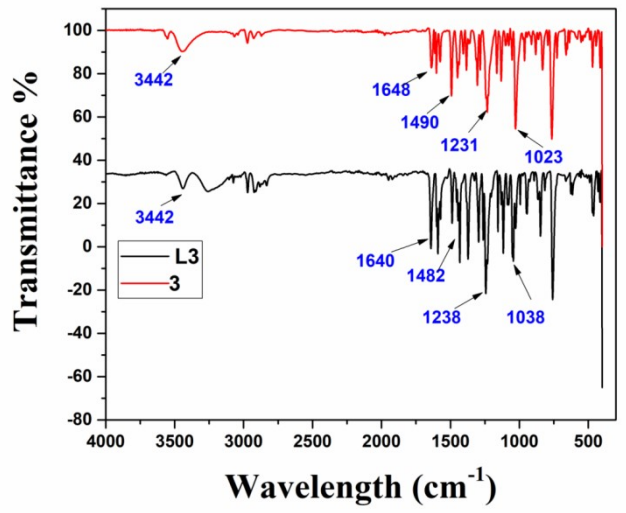

Fig. S5. IR spectrum of **L3** and **3.**

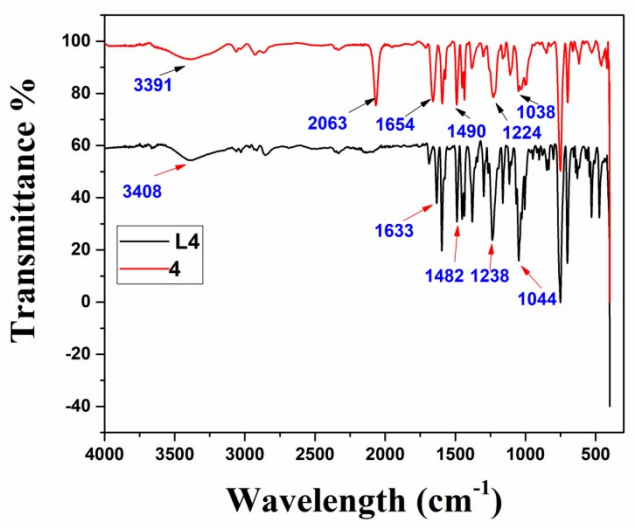

Fig. S6. IR spectrum of **L4** and **4.**

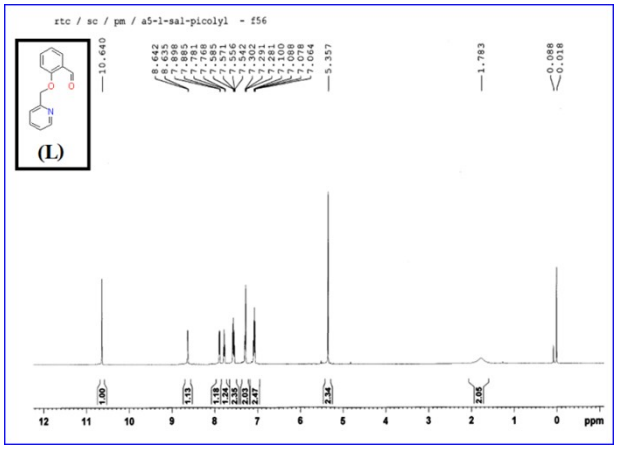

Fig. S7 ^{1}H NMR of **L.**

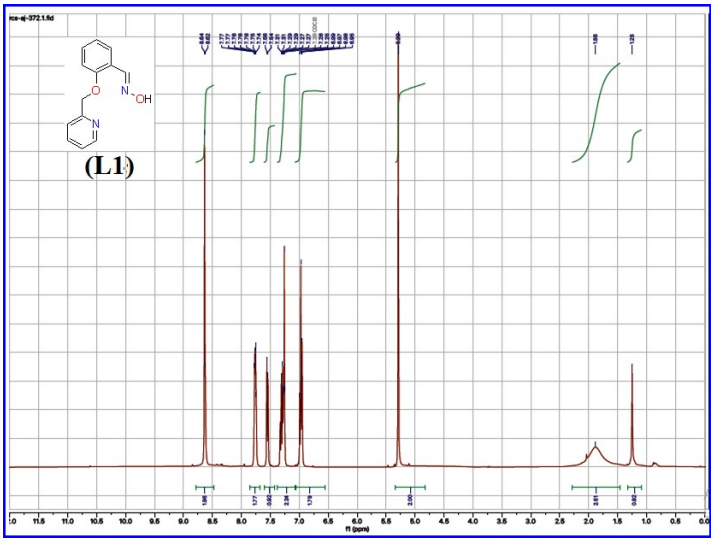

Fig. S8 ^{1}H NMR of **L1.**

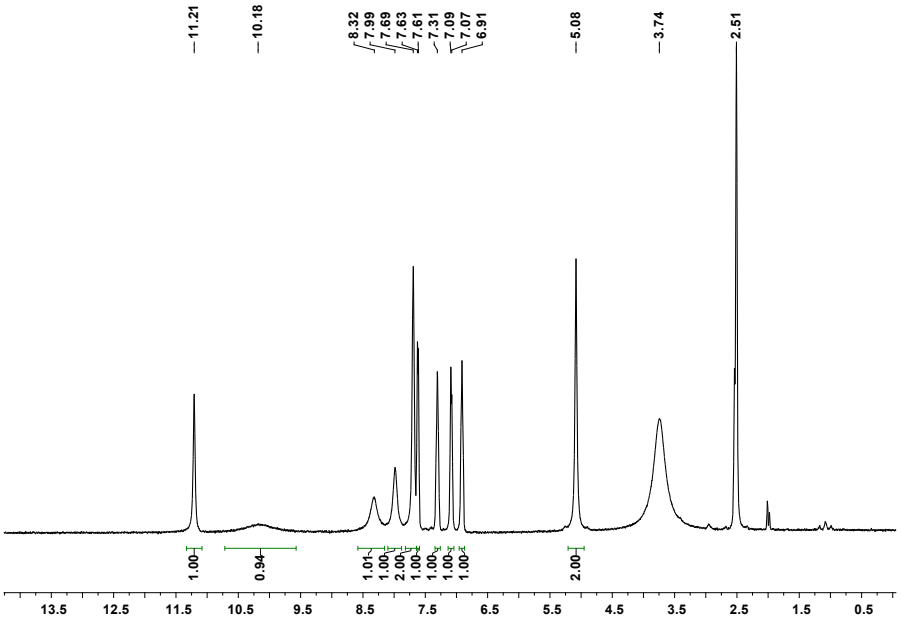

Fig. S9. ^{1}H NMR of **C1**

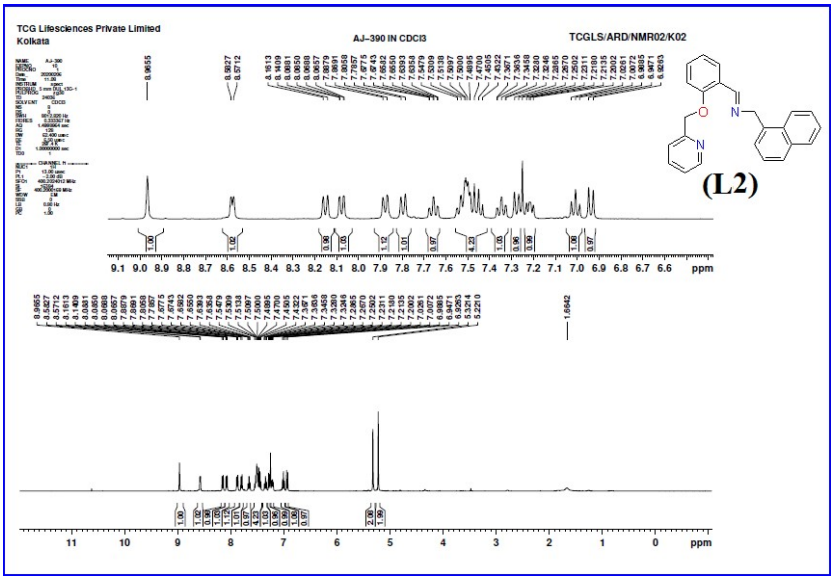

Fig. S10. ^{1}H NMR of **L2.**

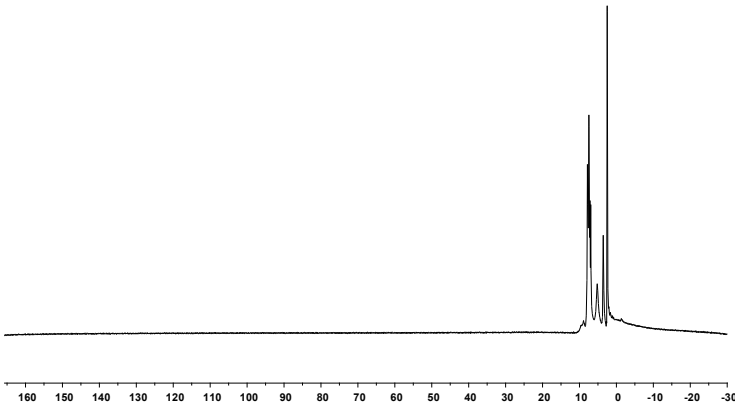

Fig. S11. ^{1}H NMR of **C2.**

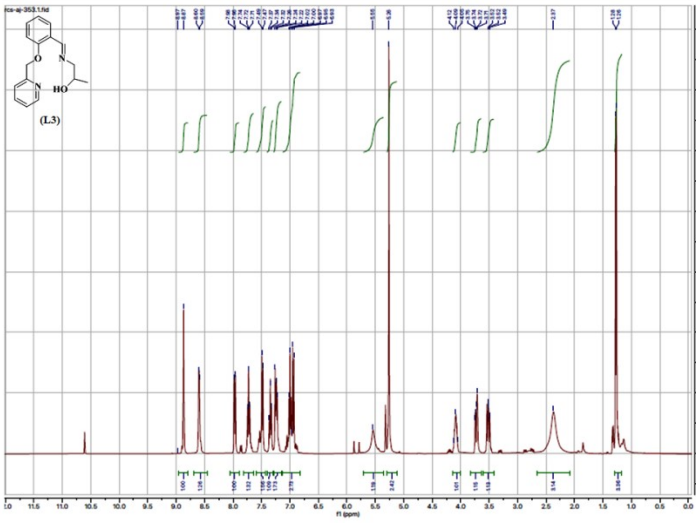

Fig. S12. ^{1}H NMR spectrum of **L3**

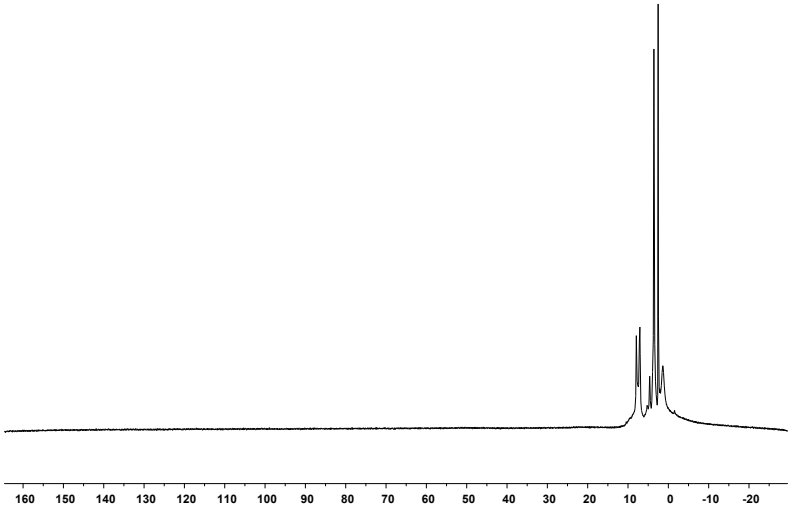

Fig. S13. ^{1}H NMR spectrum of **C3.**

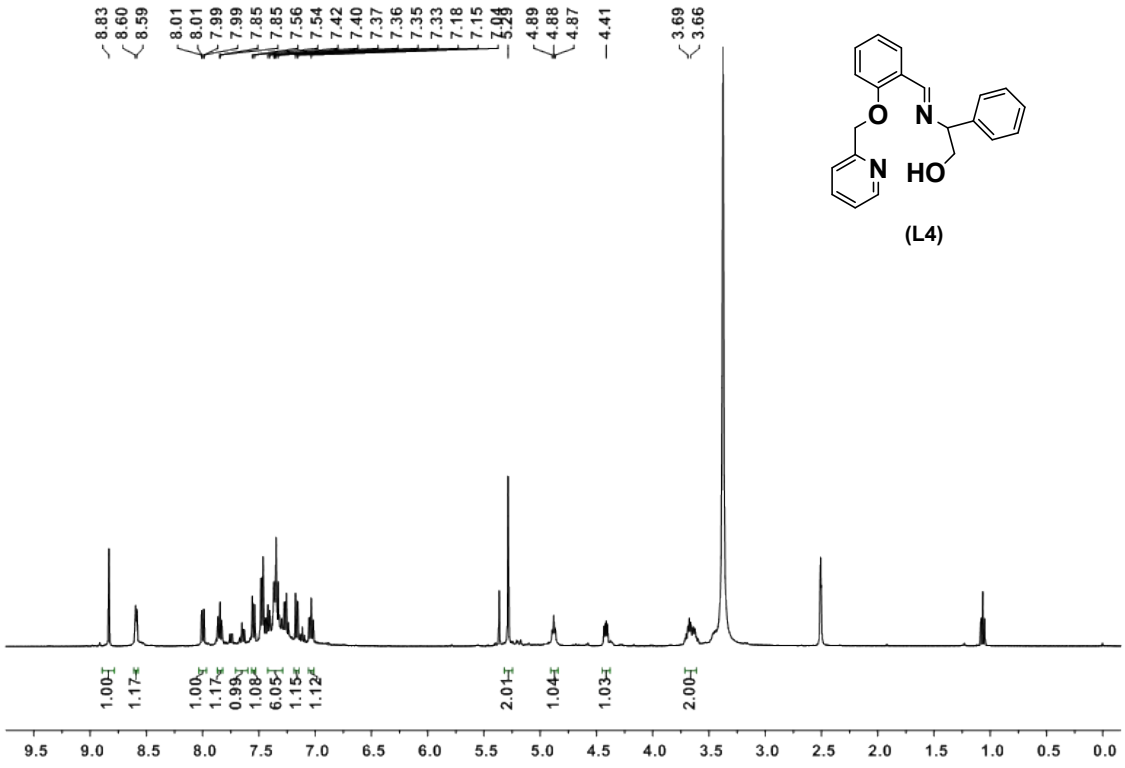

Fig.S14. ^{1}H NMR spectrum of **L4**.

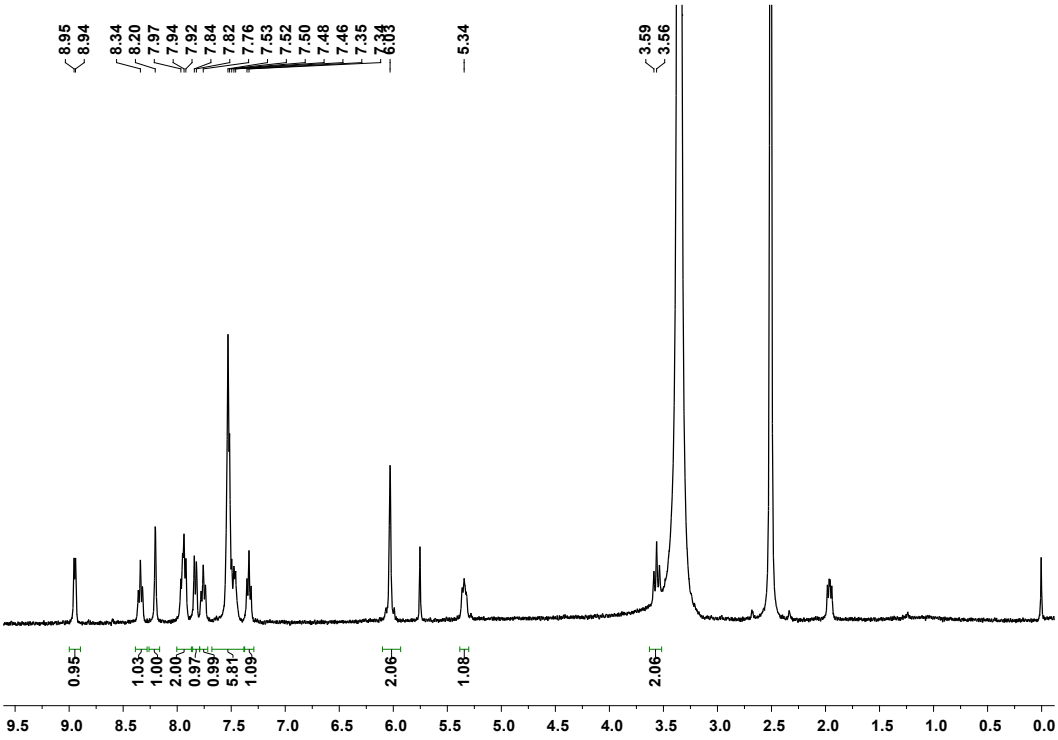

Fig.S15. ^{1}H NMR spectrum of **C4**.

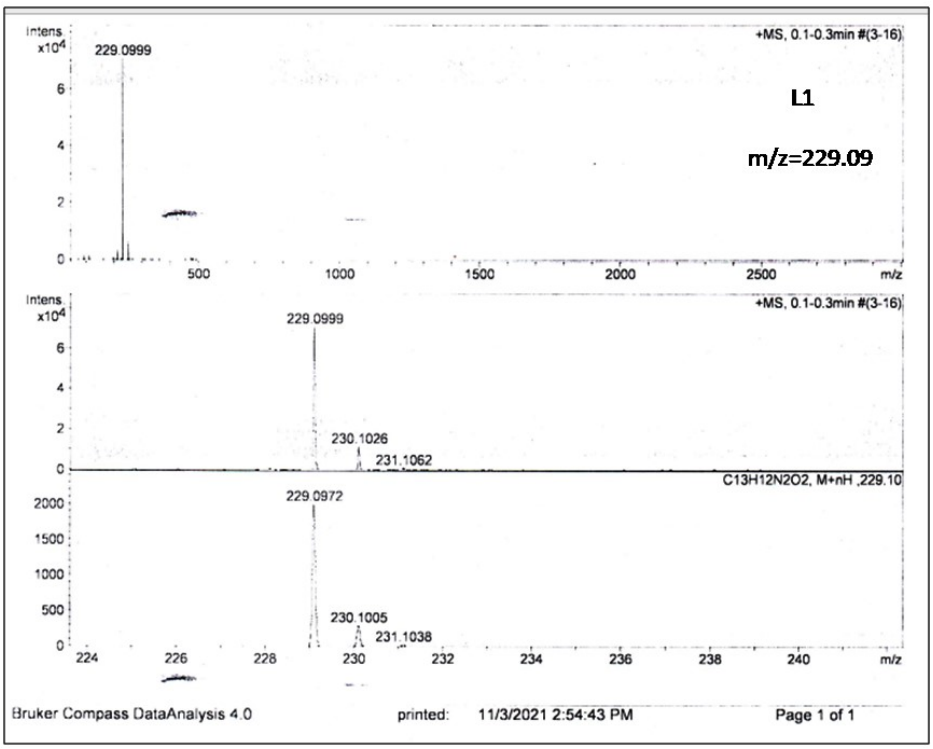

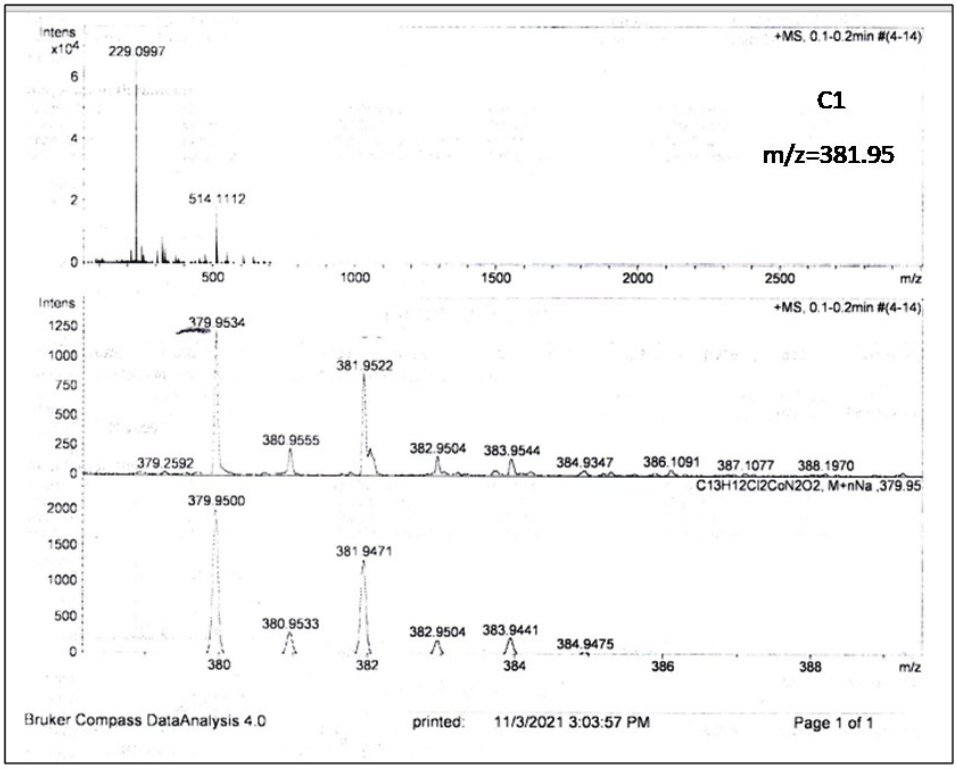

Fig. S16 Mass spectrum of **L1** and **C1**

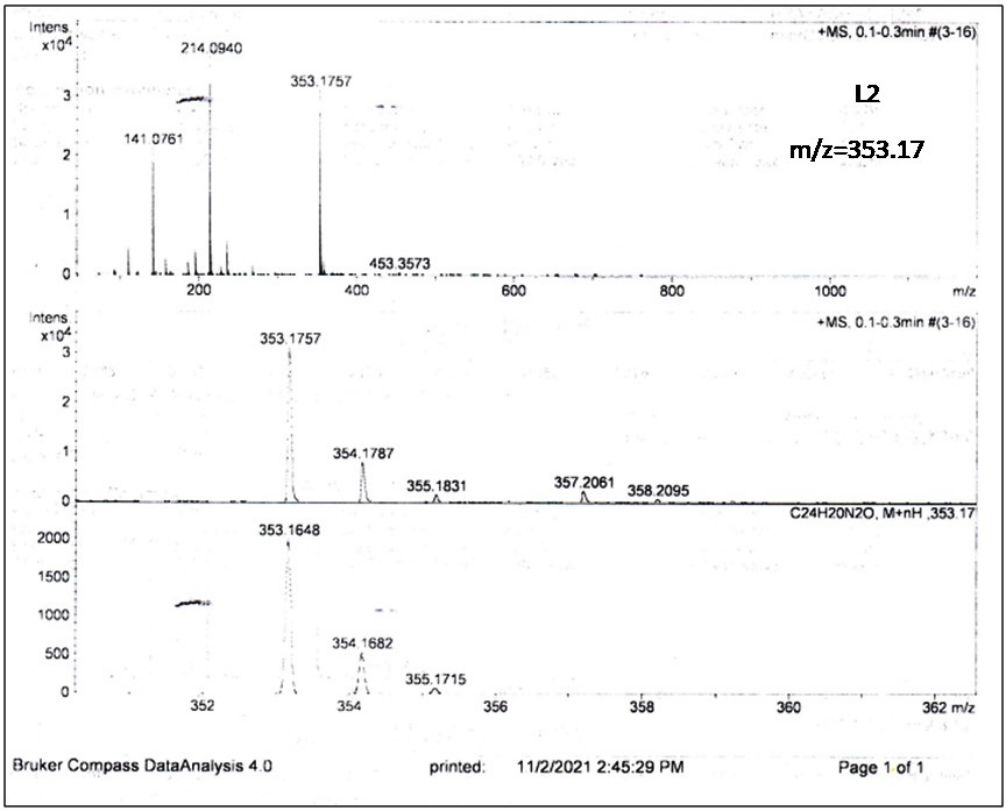

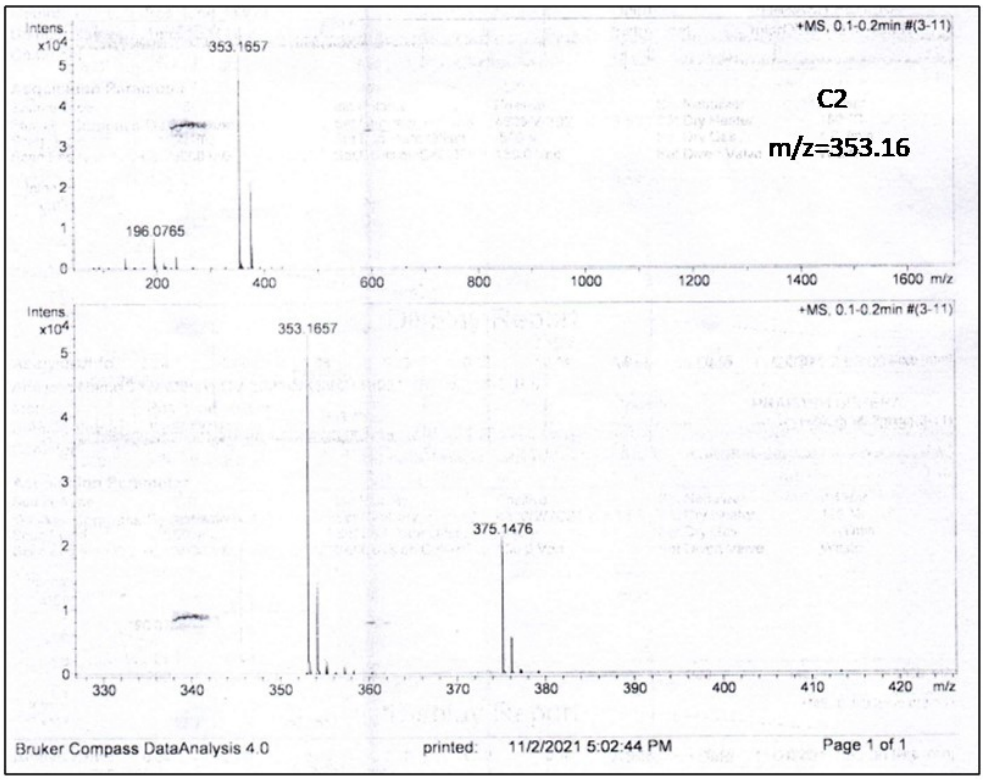

Fig. S17 Mass spectrum of **L2** and **C2**

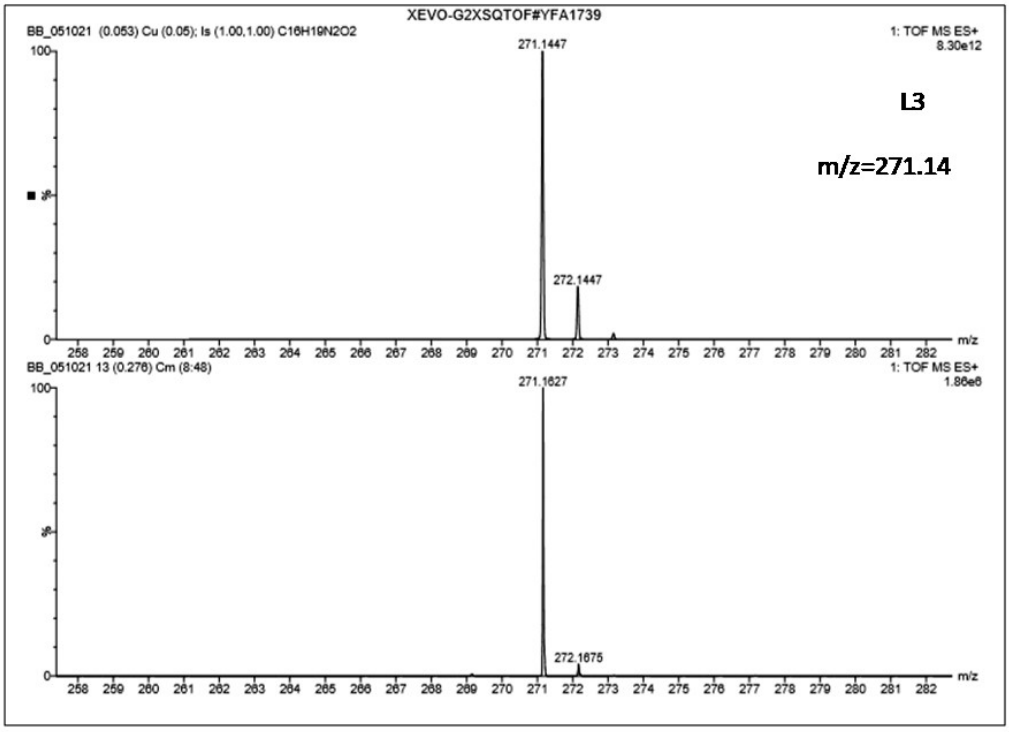

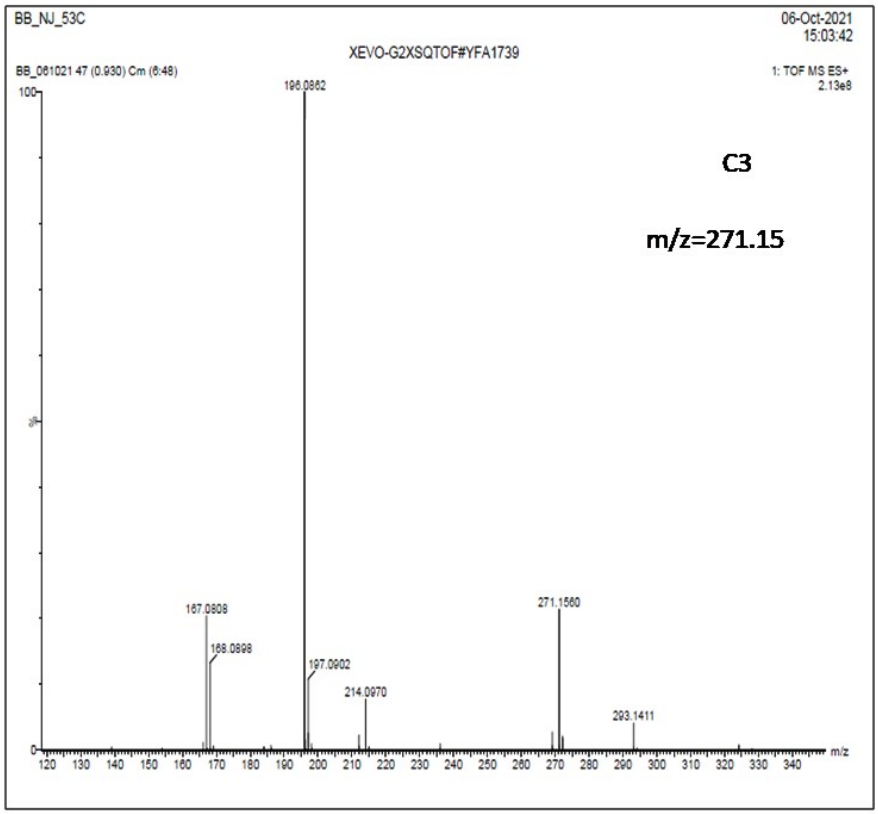

Fig. S18 Mass spectrum of **L3** and **C3**

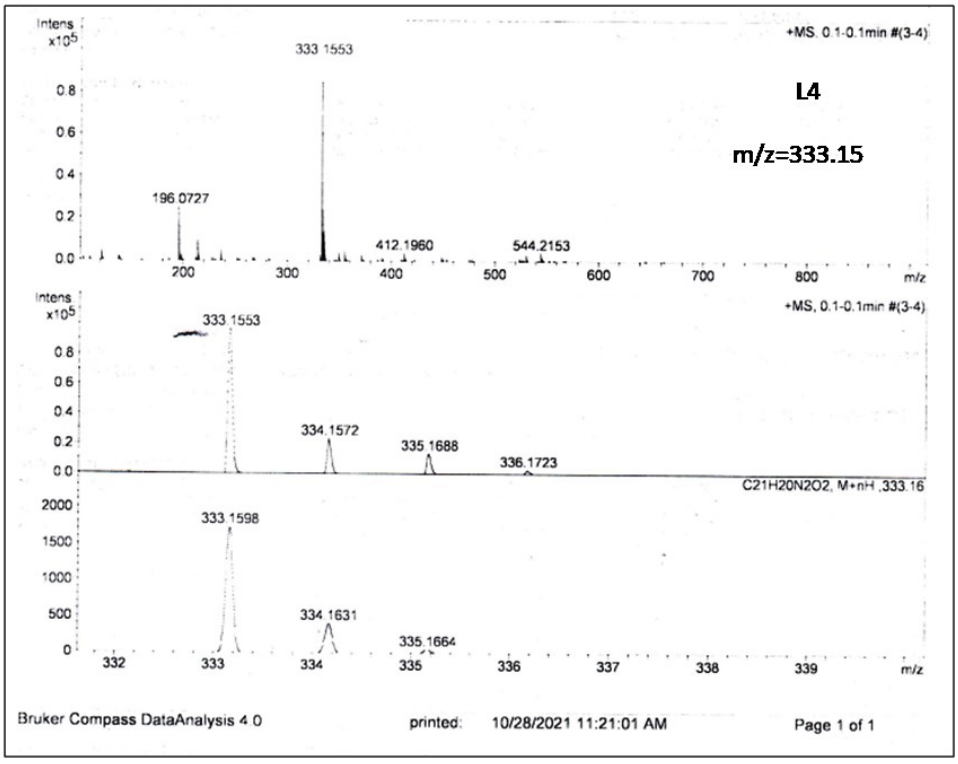

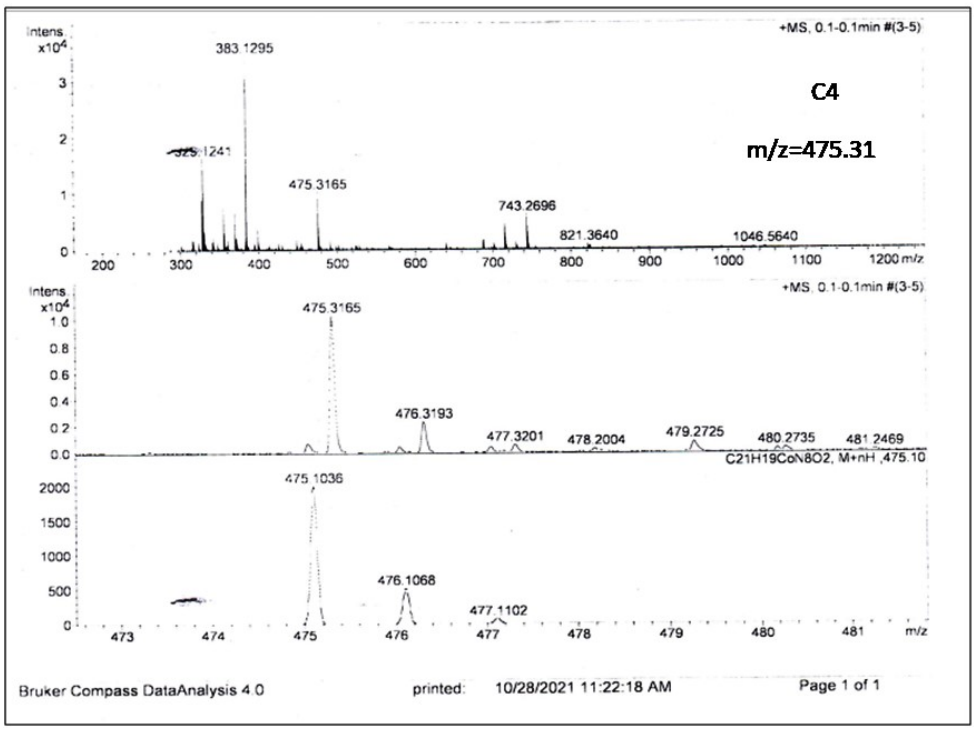

Fig. S19 Mass spectrum of **L4** and **C4**

B. X-ray Crystallography

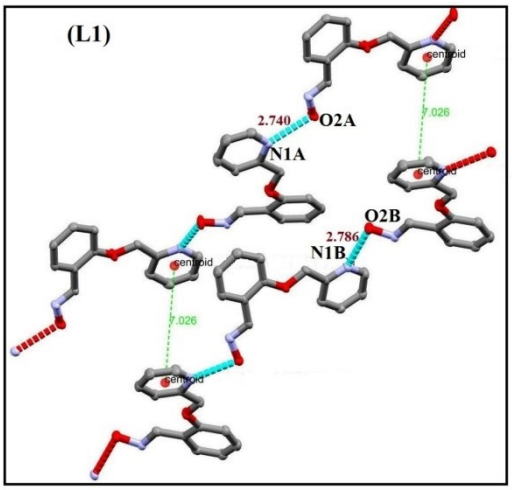

Fig. S20. The hydrogen bonding and Π−Π interaction of **L1**.

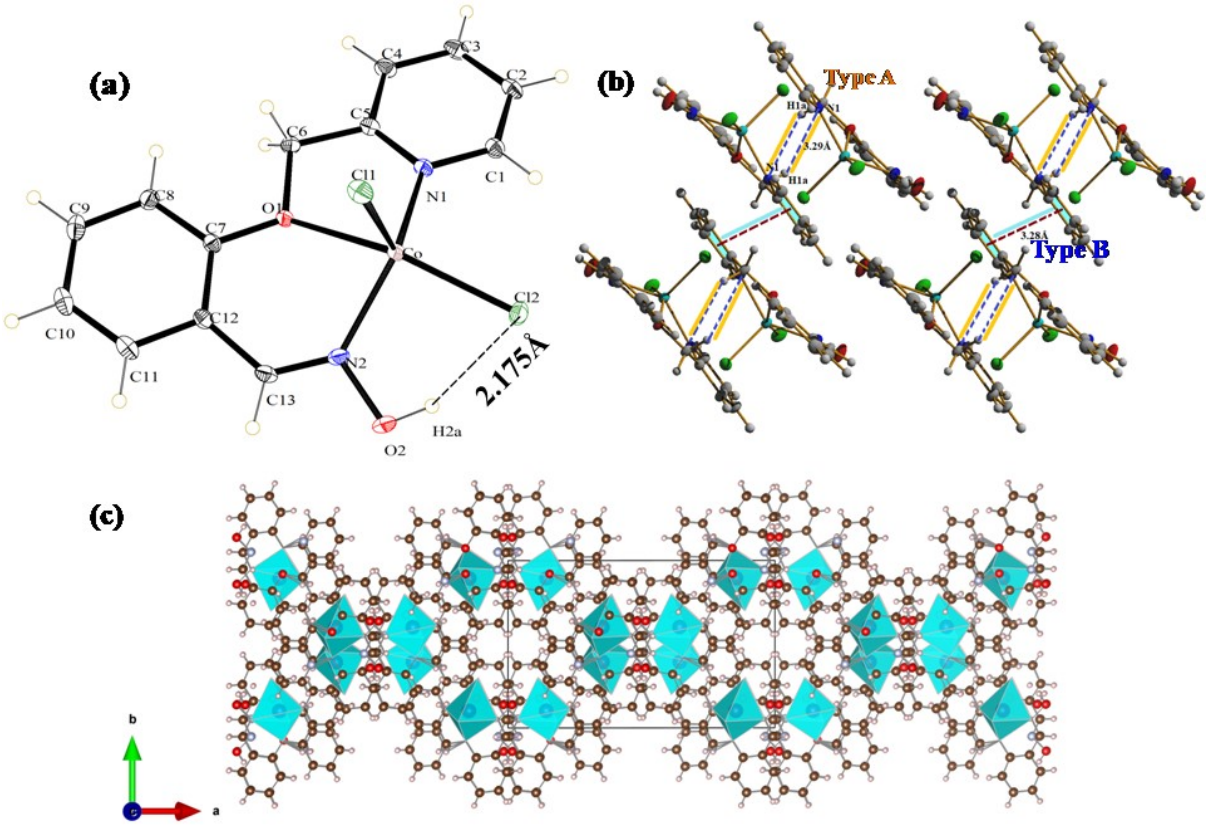

Fig. S21. (a) Intermolecular hydrogen-bonding interactions of **1**, (b) the supramolecular dimer formed by Type-A CH···π interaction of **1,** the supramolecular dimer formed by Type-B π···π interaction of **1,** (c) the extended 2D supramolecular framework in crystallographic *ab* plane with polyhedron.

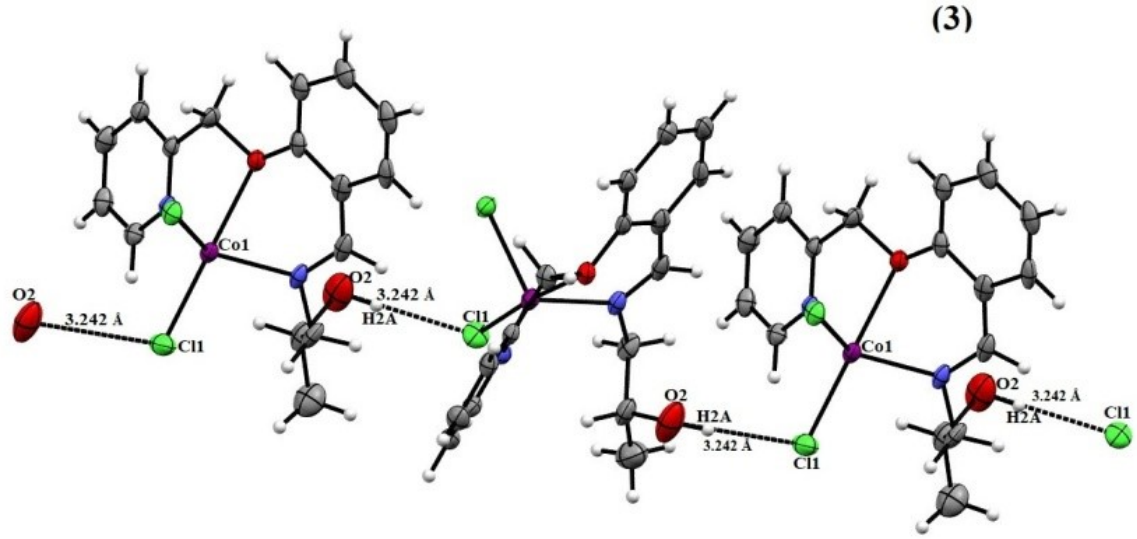

Fig. S22. The extended 1-D supramolecular sheet of complex **3**.

C. DFT study

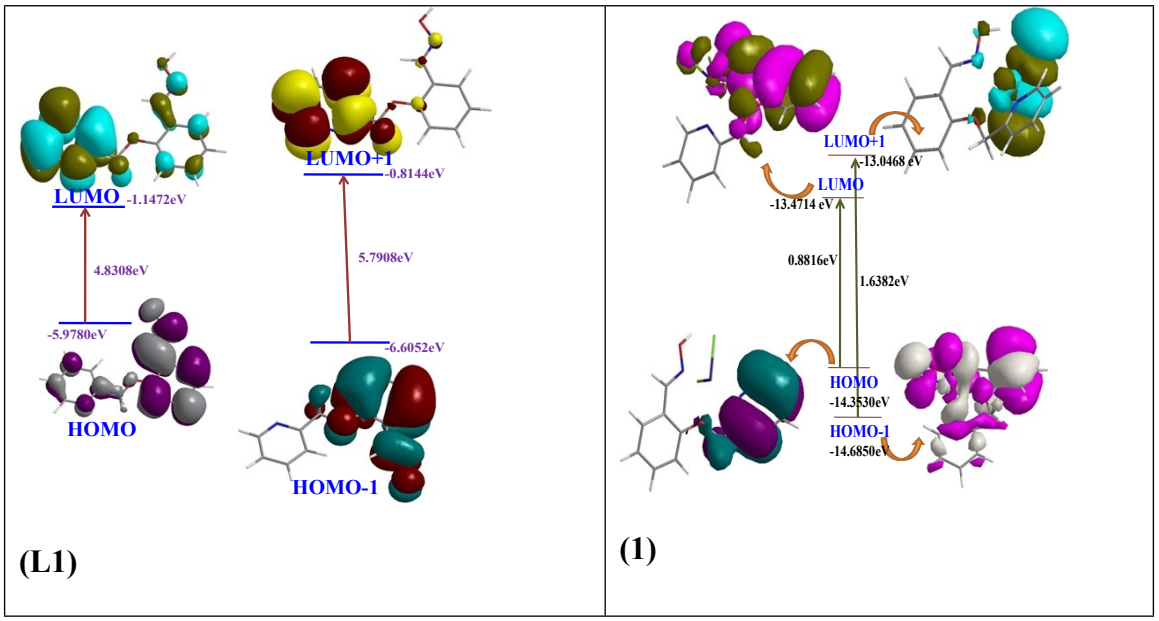

Fig. S23. Frontier molecular energy diagram comparing the energy levels of **L1** and **1**.

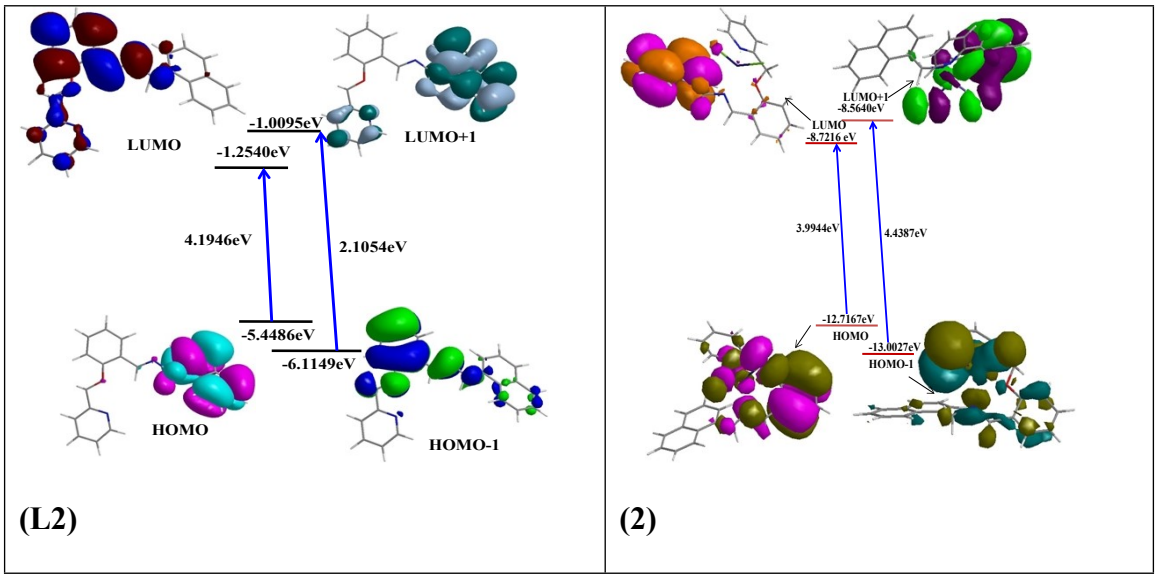

Fig. S24. Frontier molecular energy diagram comparing the energy levels of **L2** and **2**.

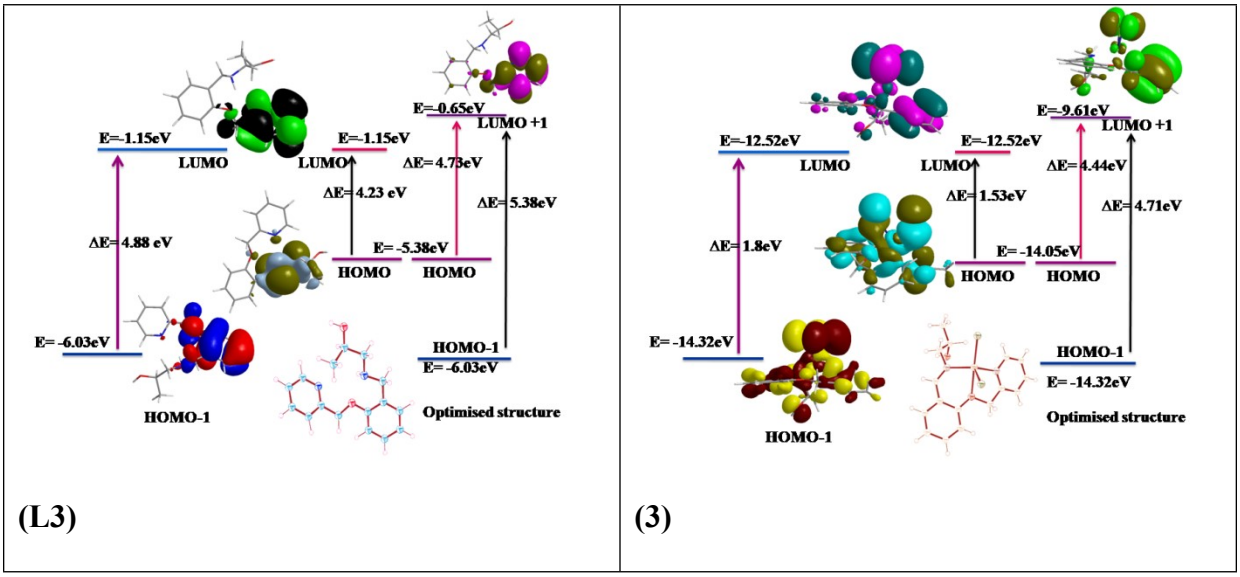

Fig. S25. Frontier molecular energy diagram comparing the energy levels of **L3** and **3**.

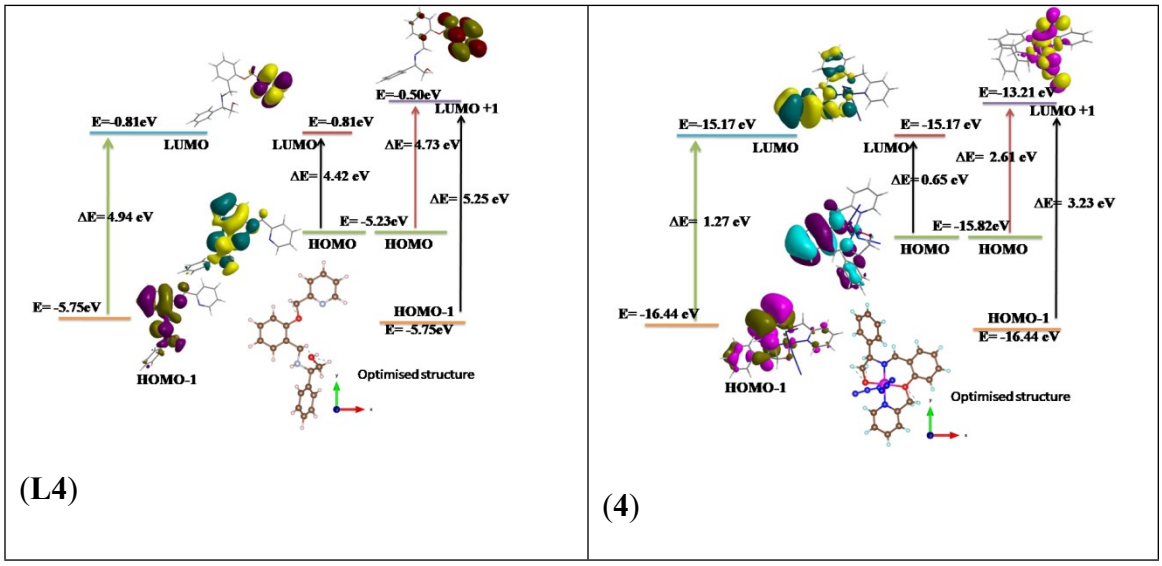

Fig. S26. Frontier molecular energy diagram comparing the energy levels of **L4** and **4**.

D. Cyclovoltammetry

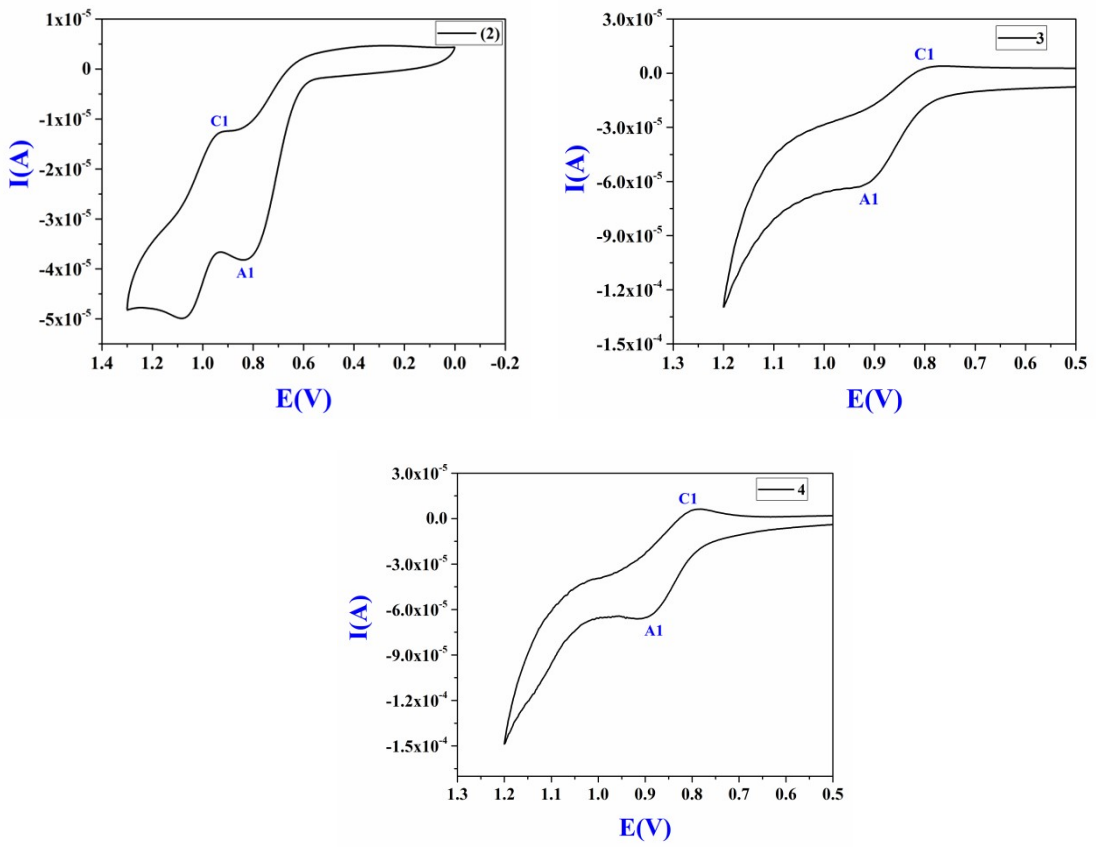

Fig. S27. Cyclic voltammogram of **2, 3** and **4.**

D. Biological study

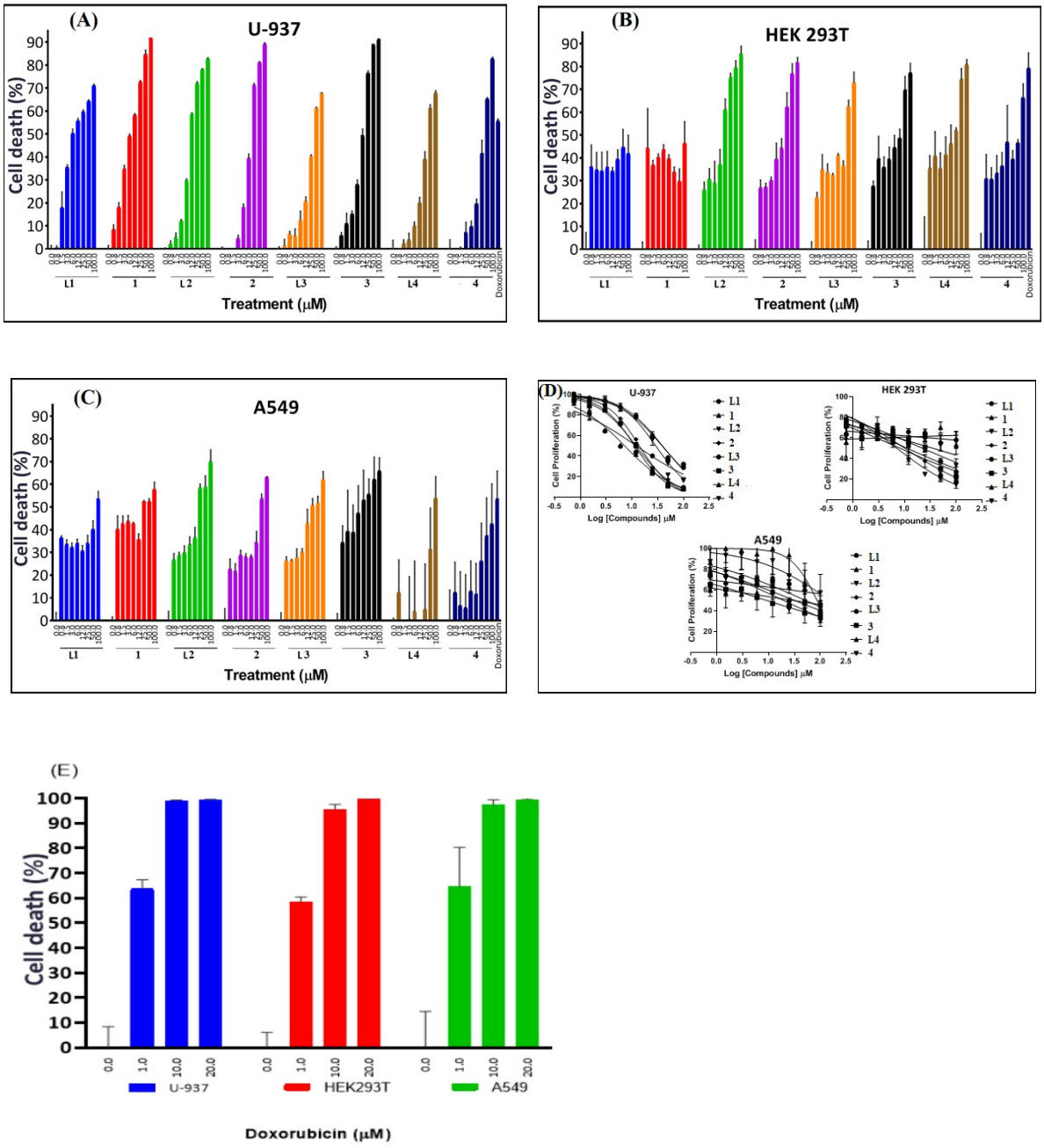

Fig. S28. A-C) Cytotoxicity effect of the compound with MTT assay: U-937, HEK 293T, and A549 cells were treated with different concentrations of L1−4, and its metal complexes 1−4 for 72 hours to study the cytotoxic effect on cell lines from different cell origin. The mean cell death from three independent experiments was calculated and represented as % cell death compared to control (taken as zero) and doxorubicin (taken as positive control). D) The data obtained was transformed, normalized and plotted as non-linear regression curve to calculate IC_{50} values using Graphpad Prism 8. E) U-937, HEK 293T, and A549 cells were treated with different concentrations of doxorubicin for 72 h and MTT assay was carried out.

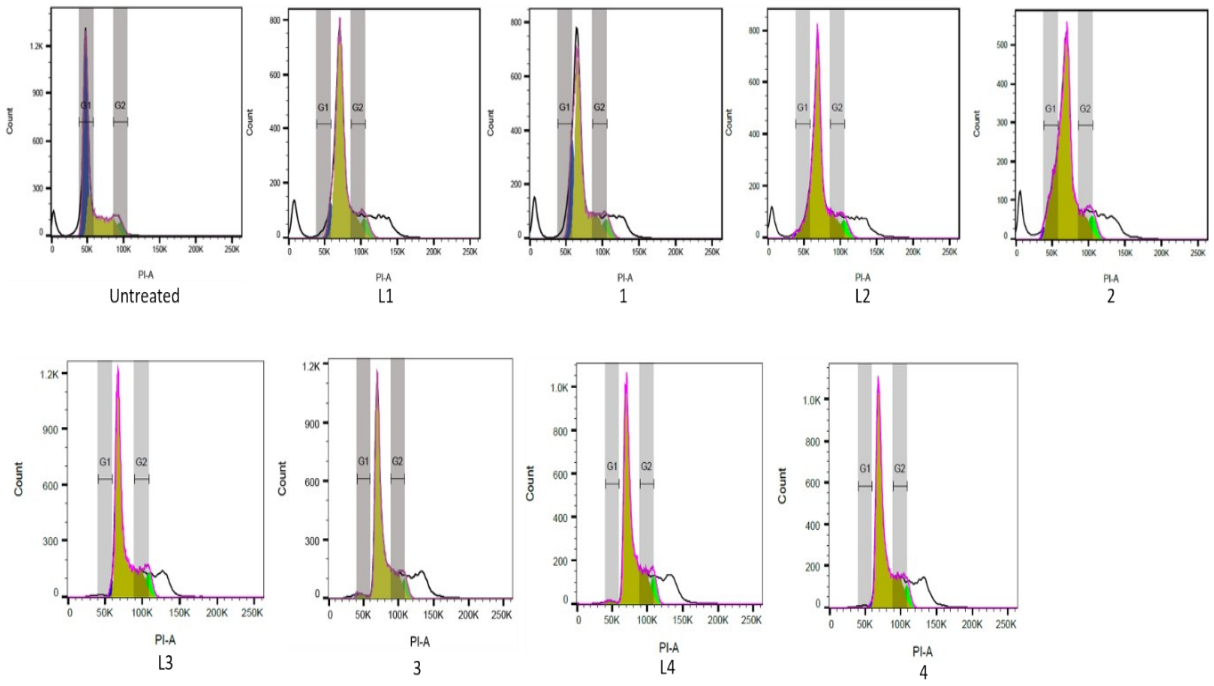

Fig. S29: The cell cycle profile studies of L1−4, and its metal complexes 1−4 with FACS.